

Article

A Theoretical Study on the Electronic Structure and Floatability of Rare Earth Elements (La, Ce, Nd and Y) Bearing Fluorapatite

Xianchen Wang ^{1,2,3} , Qin Zhang ^{2,3,4,*}, Song Mao ^{1,2,3} and Wei Cheng ^{2,3,4}¹ College of Resources and Environmental Engineering, Guizhou University, Guiyang 550025, China² College of Mining, Guizhou University, Guiyang 550025, China³ National & Local Joint Laboratory of Engineering for Effective Utilization of Regional Mineral Resources from Karst Areas, Guiyang 550025, China⁴ Guizhou Key Laboratory of Comprehensive Utilization of Non-metallic Mineral Resources, Guiyang 550025, China

* Correspondence: qzhang@gzu.edu.cn; Tel.: +86-851-8829-2081

Received: 6 July 2019; Accepted: 17 August 2019; Published: 20 August 2019



Abstract: Calcium atoms are often replaced by rare earth elements (REEs) in the lattice of fluorapatite ($\text{Ca}_{10}\text{F}_2(\text{PO}_4)_6$), making the phosphate ore an important potential rare earth resource. In this paper, the electronic properties of REEs (La, Ce, Nd and Y) bearing fluorapatite crystals have been investigated by density functional theory. Results of calculation indicated that the existence of REEs increased the cell parameters of fluorapatite in varying degrees. The REEs substitution made the Fermi level of fluorapatite to move to higher energy levels, making it easier to accept electrons. Except for Y, all the other REEs (La, Ce and Nd) showed that the electronic state mainly exists in the valence band. The Fermi level of REEs were mainly contributed by La5d, Ce4f, Nd4f and Y4d, respectively. The Mulliken values of REE–F and REE–O bonds in REEs-bearing fluorapatites were larger than those of Ca–F and Ca–O bonds in the perfect crystal, and the values of Y–F and Y–O bonds were the largest. The results of interaction between fluorapatite and oleic acid by frontier molecular orbital analysis suggested that the substitution of REEs can improve the reactivity of fluorapatite with oleic acid.

Keywords: fluorapatite; rare earth element; electronic structure; floatability; density functional theory

1. Introduction

Rare earth elements (REEs), as defined by the International Union of Pure and Applied Chemistry, contain a set of 17 chemical elements in the periodic table, specifically the 15 lanthanides, as well as scandium and yttrium [1]. REEs have been widely used in the fields of glass, chemical, petroleum, textiles, ceramics, permanent magnet materials, metallurgy, etc. [2,3]. The rare earth has become an extremely important strategic resource now, and the value of it will be more and more important with the development of science and technology [4]. REEs in nature can form independent minerals such as monazite and bastnaesite, and can also co-exists with other minerals as isomorphic substituents [5], such as rare earth-bearing apatite, one of the important potential rare earth resources [6,7].

In the phosphate rock, most of the REEs were indeed discovered. However, current researches indicated that the REE-bearing phosphates are richer in lanthanum (La), cerium (Ce), neodymium (Nd) and yttrium (Y) [8,9]. For example, for the Zhijin Xinhua rare earth phosphate deposits in western China (the largest rare earth resources reserve of phosphate rock [10]), the average grade of rare earth oxide (REO) is 0.05% to 0.13%, and La, Ce, Nd and Y account for 81.20% of the total REOs [11]. Test data [12,13] showed that REEs replace calcium mainly in the form of isomorphism in the phosphate rock (mainly fluorapatite or carbonate-fluorapatite). Although the apatite and dolomite or calcite

contain the same element Ca in crystals, the REEs can be only displaced into the apatite lattice rather than the dolomite or calcite, and there is no relevant explanation for that. Research on occupancy and spectral behavior of REEs in apatite structures has been quite active [14–18]. According to the results of structure determination, light REEs mainly occupied the smaller Ca2 site [12,19]. According to the results of calculated valence parameters based on bond strength and bond distance [20], fluorapatite is insufficient at the Ca2 site, but excessive at the Ca1 site, so REE^{3+} tends to occupy the Ca2 site to compensate for the insufficiency of bond valence. The spectrometric determination of synthetic samples supported the above conclusion of the crystal structure studies [14,15].

The density functional theory (DFT) is a computational quantum mechanical modelling method used in physics, chemistry and materials science to investigate the electronic structure of many-body systems, in particular atoms, molecules and the condensed phases. So far, DFT has been widely used in the study of the effect of lattice impurity substitution on the electronic structure, surface properties and flotation properties of minerals [21–25], especially sulfide ores [26–31]. Chen et al. investigated the effects of four impurities (Ag, Bi, Sb and Zn) on the electrochemical adsorption of butyl xanthate on a galena surface [28], and studied the influences of vacancy defects of galena [32] and pyrite [31] on their electronic structure and flotation. Ye et al. studied the flotation behavior of three typical impurities (Fe, Cu and Cd) bearing sphalerite [29], and synthetic impurities (Cu and Cd) bearing ZnS [30]. Among these researches, it was found that almost all the impurities changed the electronic structures of minerals, such as the lattice parameter, Fermi energy, even semiconductor type. Further, the adsorption of oxygen molecule (O_2) on galena (100) surfaces containing Ag, Cu, Bi, and Mn impurities was investigated, and it was found that the impurities could change the semiconductor electronic structure of galena surface and influence the adsorption of oxygen molecules on it [27]. For other minerals, Gao et al. [33] studied the electronic structure of fluorite substituted by REEs (Ce, Th, U and Y) at the calcium site. Besides that, de Leeuw [21] studied the absorption and distribution characteristics of chloride ions in fluorapatite structure by theoretical calculation. However, the influence of REEs on the electronic structure and surface properties of fluorapatite crystals has not been systematically and thoroughly studied.

On the other hand, apatite and its associated gangue minerals, such as dolomite and calcite, are usually separated by flotation [34–37]. The traditional collector for apatite flotation is fatty acids (such as oleic acid) and its salt [25,38,39]. In this process, the floatability of minerals depends on many properties, but most fundamentally on the surface properties, which have been studied and attempted by many researchers using different aspects, such as zeta potential and the isoelectric point [35]. Lattice defects of mineral have a great influence on their surface properties, which can change the lattice parameters of crystal, Fermi energy, electronic structure and frontier orbitals [29,33]. The mineral crystallinity and impurity may also affect the mineral dissolution, influence collector adsorption and may lead to different flotation results [34]. The presence of impurities in crystals significantly changed the semiconductor properties of minerals, thus affecting the electrochemical behavior of sulfide minerals interacting with xanthate, and even changing the surface products of minerals. The interaction of xanthate with sphalerite containing cadmium and copper produced double xanthate, but no double xanthate was found on sphalerite containing iron [30]. When galena contains silver, antimony and copper impurities, its floatability became better, and when it contains zinc, manganese and antimony impurities, its floatability decreased [28]. It could be inferred that the addition of REEs (La, Ce, Nd and Y) to fluorapatite crystals may lead to different electronic structures and the floatability of apatite.

In this study, the DFT calculations were employed to investigate the effect of REEs lattice impurities (La, Ce, Nd and Y) on the electronic structures of fluorapatite, and the influence of REEs on the reactivity of fluorapatite with oleic acid was predicted.

2. Computational Models and Methods

The lattice parameter of perfect fluorapatite (P-FAP) crystal was obtained from the literature [40]. The symmetry group of fluorapatite crystal is L6PC. The unit cell consists of ten Ca atoms, two F atoms, and six (PO₄) groups, and the cell parameters are $a = b = 9.397 \text{ \AA}$, $c = 6.878 \text{ \AA}$, and $\alpha = \beta = 90^\circ$, $\gamma = 120^\circ$. As we can see in Figure 1a, there are two positions of Ca atoms in unit cell. The Ca1 atoms locate in the center of six phospho-tetrahedrons at upper and lower layers, and collected with nine O atoms in the vertices of six phospho-tetrahedrons. This special structure leads to a quite large channel parallel to the c-axis [12]. The two F atoms located in the channel form a coordination octahedron with the six Ca2 atoms of the upper and lower layers. The Ca atoms at the top corner of coordination octahedron are connected to F atoms in channel and the O atoms at top corner of the adjacent four phospho-tetrahedrons. The coordination number of Ca2 atom is seven. Ratio of Ca1 and Ca2 is 4:6. The crystal of REE-bearing fluorapatite (REE-FAP) was obtained by substituting a rare earth atom for a Ca2 atom at a specific position in the fluorapatite crystal. The models of the P-FAP and REE-FAP crystals are shown in Figure 1 (the corresponding atomic number is marked inside).

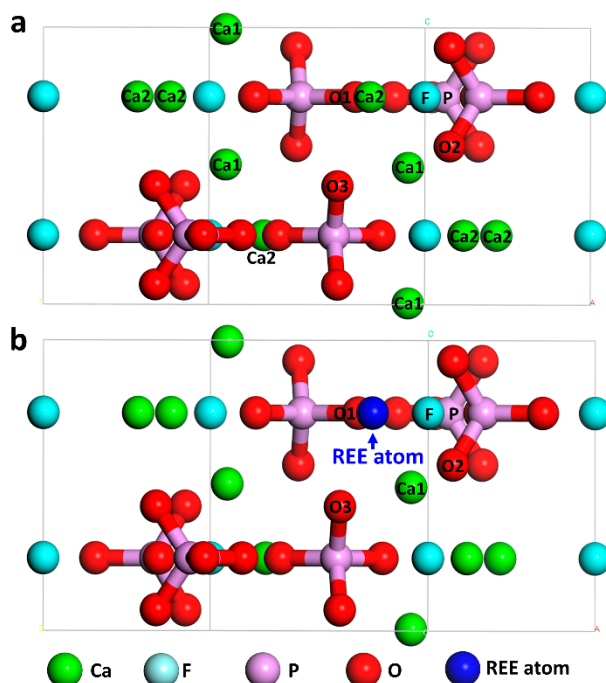


Figure 1. Models of perfect (a) and rare earth element (REE)-bearing fluorapatite crystals (b).

DFT calculations were performed using the program CASTEP and Dmol³ (Material Studio 6.1, Accelrys, San Diego, USA). The calculations of geometry optimization and electronic properties on fluorapatite were performed using Cambridge Serial Total Energy Package (CASTEP) [41] employing plane wave (PW) basis sets, which is a first-principle pseudopotential method based on DFT. Ultra-soft pseudopotential was used to describe electron–ion interactions. The generalized gradient approximation (GGA) [42] developed by Perdew–Wang generalized-gradient approximation (PW91) [43] was employed as the exchange correlation functional. The plane wave cutoff energy of 480 eV and special k-point sampling density of $2 \times 2 \times 4$ grid were chosen. The valence electron configurations considered in the work were O $2s^2 2p^4$, F $2s^2 2p^5$, P $3s^2 3p^3$, Ca $3s^2 3p^6 4s^2$, La $5s^2 5p^6 5d^1 6s^2$, Ce $4f^1 5s^2 5p^6 5d^1 6s^2$, Nd $4f^4 5s^2 5p^6 6s^2$ and Y $4d^1 5s^2$. The fluorapatite cell parameters obtained after minimization were $a = b = 9.455 \text{ \AA}$, $c = 6.888 \text{ \AA}$, with errors of 0.61% and 0.15%, respectively, compared with experiment values [30]. And the stable structure of fluorapatite crystal can be obtained with a relatively low total energy of $-22,996.01 \text{ eV}$. This all shows that the calculation conditions chosen were sufficient for the system. Both the Fermi energy and frontier orbitals of fluorapatite were calculated

by DMol³ with a single-point energy method after optimization with the same setting parameters as CASTEP. Both the structure optimization and frontier orbital calculations of oleic acid were performed using Dmol³ with GGA-PW91 functional, DNP (double numerical basis + polarized basis) basis set (basis file of 3.5), effective core potentials, a fine quality (global orbital cutoff of 5.5 Å), and SCF tolerance of 1.0×10^{-6} eV/atom. The X-ray powder diffraction of crystals were performed using powder diffraction calculation in Reflex module (Material Studio 6.1, Accelrys, San Diego, USA). The range of 2-theta was set at 10–90°, and step size was set at 0.05°.

3. Results and Discussion

3.1. Substitution Energy and Lattice Parameter

Impurity substitution energy refers to the energy required by impurity atoms to replace lattice atoms. In this paper, the substitution energy of a rare earth atom R (La, Ce, Nd and Y) for one Ca atom in bulk fluorapatite is defined and calculated by the following formula [29,31,32]:

$$\Delta E = E_{\text{REE}}^{\text{total}} + E_{\text{Ca}} - E_{\text{perfect}}^{\text{total}} - E_{\text{REE}} \quad (1)$$

where $E_{\text{REE}}^{\text{total}}$ represents total energy of fluorapatite containing rare earth atom substitution, and $E_{\text{perfect}}^{\text{total}}$ represents the total energy of a perfect fluorapatite of the same size as that of a REE-FAP. E_{Ca} and E_{REE} represent the calculated total energy of one Ca atom and one REE atom, respectively. The isolated Ca or REE atom was placed inside a $10 \text{ \AA} \times 10 \text{ \AA} \times 10 \text{ \AA}$ cubic cell, and the total energy was obtained under the same calculation parameters as fluorapatite bulk optimization. A negative value for energy indicates that the substitution reaction is prone to occur, while a positive value means that it may not have occurred. If the negative value of ΔE is larger, it indicates that the substitution reaction is more likely to occur. The substitution energies of REE atoms substituting for Ca2 atom in fluorapatite are shown in Figure 2.

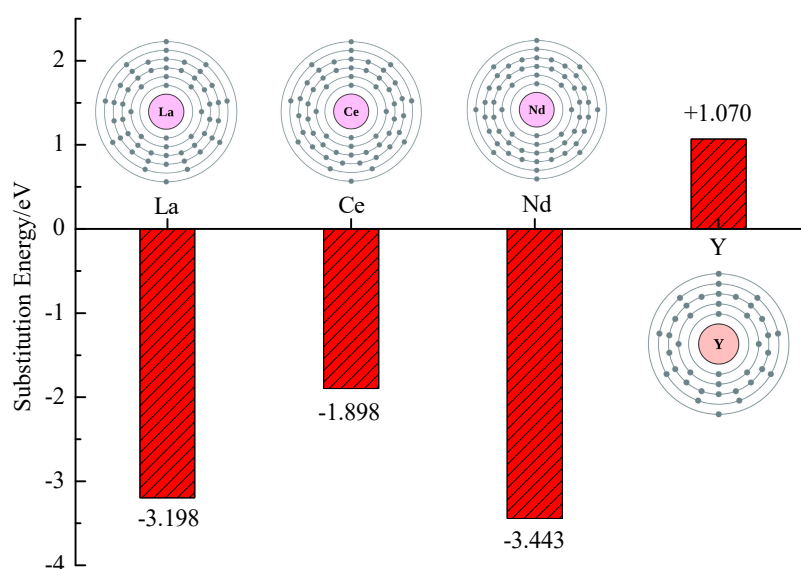


Figure 2. Substitution energies of REE atoms substituting for Ca atom.

We can see from Figure 2, the substitution energies of three light REEs (La, Ce and Nd) were negative, which indicated that these three REEs can be relatively easily substituted into the crystal lattice during the formation of the fluorapatite crystal. On the other hand, the substitution energy of heavy REE Y was positive, suggesting that the substitution of Y may have needed much more complex conditions during crystallization, such as high temperature or pressure [29,31].

The lattice parameters of P-FAP and of REE-FAP crystals are shown in Table 1. The lattice parameters of REE-FAP crystals were slightly larger than that of P-FAP, and the lattice parameters of La-FAP were the largest among them. The reason for the swelling of REE-FAP crystals may be related to the atomic radius or covalent radius and electronegativity of REE atoms, and the spin characteristics of rare earth atoms were also one of the reasons that affect the lattice parameters compared to the calcium atom in the original cell [15]. In addition to the trivalent REE³⁺, the bivalent Sr²⁺, Mn²⁺, Fe²⁺, and Ba²⁺, and monovalent ions such as Na⁺ are often present. It is generally believed that the substitution of these cations will lead to different degrees of aberration of apatite crystal cells based on the crystal structure studies [14]. Since the presence of impurity atoms in the mineral unit cell rebalanced the lattice of the unit cell, the unit cell volume of the mineral expands or shrinks, causing the mineral unit cell to deviate from the ideal form to form a unit cell distortion. In general, lattice expansion could lead to lattice distortions that change the electronic structure of fluorapatite, which was also explained by the studies of sphalerite [29] and galena [27]. Ferrer et al. [44] also found that the unit cell parameters of pyrite increased with the increase of nickel impurity concentration by X-ray powder diffraction (XRPD) tests.

Table 1. Lattice parameters of perfect fluorapatite (P-FAP) and of REE-bearing fluorapatite (REE-FAP) crystals.

Fluorapatite Type	Lattice Parameter/Å					
	<i>a</i>	$\Delta a/\%$	<i>b</i>	$\Delta b/\%$	<i>c</i>	$\Delta c/\%$
P-FAP	9.455	0	9.455	0	6.888	0
La-FAP	9.493	0.40	9.651	2.10	6.927	0.57
Ce-FAP	9.570	1.22	9.530	0.80	6.920	0.47
Nd-FAP	9.543	0.93	9.509	0.57	6.919	0.45
Y-FAP	9.506	0.54	9.515	0.64	6.929	0.60

Note: *a*, *b* and *c* are cell parameters, and the “ Δ ” representing deviations of REE-FAP from P-FAP value.

Figure 3 shows the XRPD patterns of P-FAP and REE-FAP crystals. It is difficult to compare the difference between these phases from such long-range XRPD pattern as in Figure 3a. Thus, short-range XRPD pattern focused on (211), (112), and (300) peaks at range of 30° to 33°, as shown in Figure 3b.

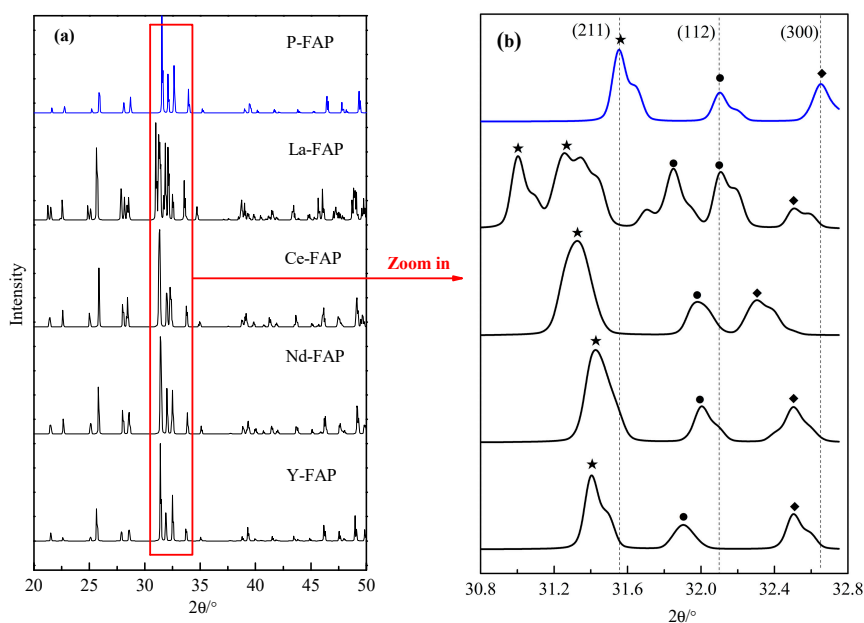


Figure 3. XRD patterns of perfect and REE-bearing fluorapatite crystals by Material Studio: (a) long-range pattern, (b) short-range pattern. (★, ● and ◆ represent (211), (112) and (300) planes, respectively).

The short-range XRPD patterns clearly revealed the pronounced changes in the 2 theta and intensity for the REE-FAP crystals compared to the P-FAP, as shown in Figure 3b. The (211), (112) and (300) peaks of all the REE-FAP crystals shifted to a slower angle with some certainty. Except Y, the intensity of XRPD peaks in La, Ce, and Nd-bearing fluorapatite were also strengthened. These results indicate that the lattice of REE-FAP crystals increased compared with P-FAP, and furtherly confirm the above analysis of lattice parameter in Table 1, which was consistent with the findings of fluorapatite by Liu et al. based on spectral analysis [14].

3.2. Fermi Level

The Fermi level can represent the highest energy level occupied by electrons in the ground state system at 0 K; it is usually equal to Fermi energy in the field of semiconductor physics, and is widely used [26]. For the band structure theory, the Fermi level is considered to be the hypothetical level of electrons, that is, the probability that the energy level is occupied is 50% at any given thermodynamic equilibrium moment, and the higher Fermi level system is more likely to transfer electrons and lower its Fermi level to make the system more stable [33] (as shown in Figure 4). The Fermi level of P-FAP and of REE-FAP crystals is also shown in Figure 4.

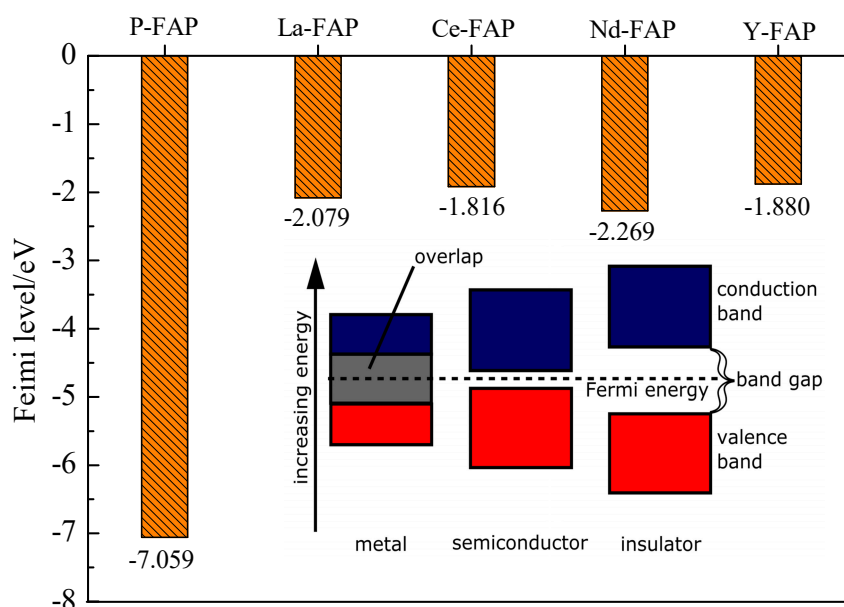


Figure 4. Fermi level of P-FAP and of REE-FAP crystals.

Figure 4 shows that the Fermi level of P-FAP is -7.059 eV. The Fermi levels of REE-FAP all increased compared to that of P-FAP, suggesting that the probability that electrons occupy quantum states was increased. In other words, the substitution of REEs made the fluorapatite crystal accept electrons more easily. Similar researches on sphalerite [29] and fluorite [33] also confirmed that the impurities made the Fermi level of mineral crystals increase.

3.3. Density of States

In solid state physics, the density of states (DOS) of a system describes the number of states that are available to be occupied by the system at each level of energy, and it is generally an average over the space and time domains of the various states occupied by the system [24]. High DOS at a specific energy level means that many states are available for occupation. The DOS of P-FAP and REE-FAP crystals is shown in Figure 5. Compared with P-FAP, the total density peaks of REE-FAP moved towards lower energy level, while the Fermi level moved towards higher energy level due to the substitution of REEs in fluorapatite crystals. It was consistent with the analysis of Fermi level

results, and suggested that the replacement of REEs makes the fluorapatite more capable of gaining electrons, that is to say, its oxidation capacity was further strengthened [40,45], which was beneficial to the interaction of fluorapatite with collectors (oleic acid) when flotation occurs.

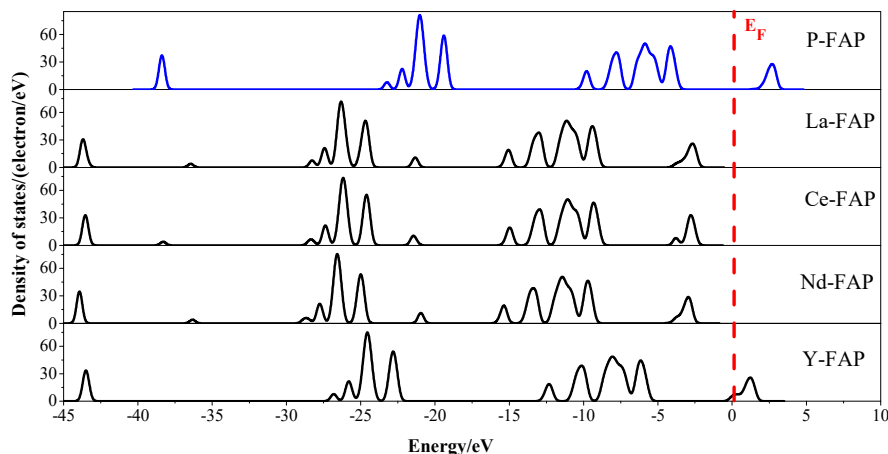


Figure 5. Density of state (DOS) of P-FAP and REE-FAP crystals.

Compared to DOS, the partial density of state (PDOS) can show the contribution of each atomic orbital. The PDOS of REE atoms in fluorapatite crystals was shown in Figure 6. The Fermi level (E_F) was referenced at 0 eV. From Figure 6, we can see clearly that all the REE atoms had the energy level occupied near the E_F . The Fermi levels of La and Y were mainly occupied by the d orbital (La5d and Y4d), while the Nd and Ce were mainly contributed by the f orbital (Ce4f and Nd4f). Besides that, in the valence band, it was found that the REE atoms La, Nd, and Ce all showed an energy level (mainly contributed by s orbital and p orbital), while the Y did not. The study on PDOS of impurity Y in fluorite reported the same opinion [33].

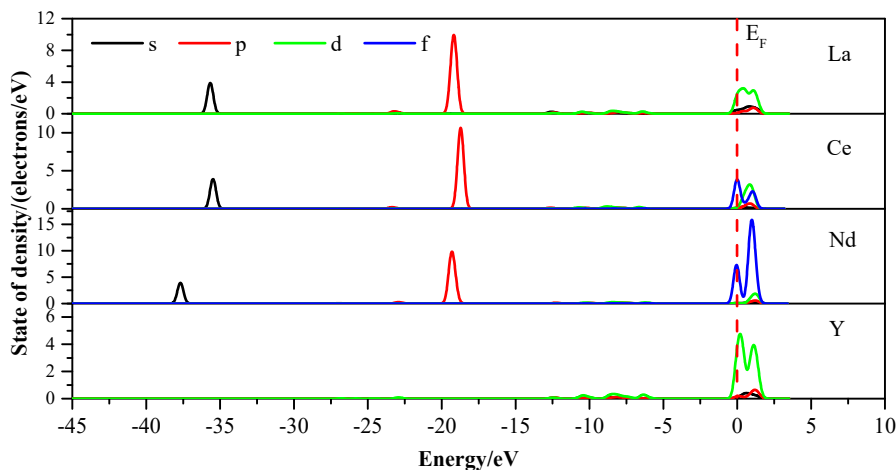


Figure 6. Partial density of state (PDOS) of rare earth atoms in REE-FAP crystals.

The PDOS of the single Ca, F, O and P atoms adjacent to the rare earth atom were shown in the Figures 7–10, respectively. From the comparative analysis in the figures, it can be clearly seen that the PDOS peaks of Ca, F, O and P atoms adjacent to rare earth atom in REE-FAP both moved to different degrees in the direction of low energy due to the substitution of REEs, which was consistent with the change trend of total DOS of fluorapatites. We can see from Figure 9 that the electronic state near the Fermi level in P-FAP was mainly contributed by the O atom (O2p), while the peak near the Fermi level was mainly contributed by the REE atom (Figure 6) and slightly provided by the Ca atom (Figure 7)

in REE-FAP, which was due to the substitution of the REE atoms making the state peak move to the lower energy.

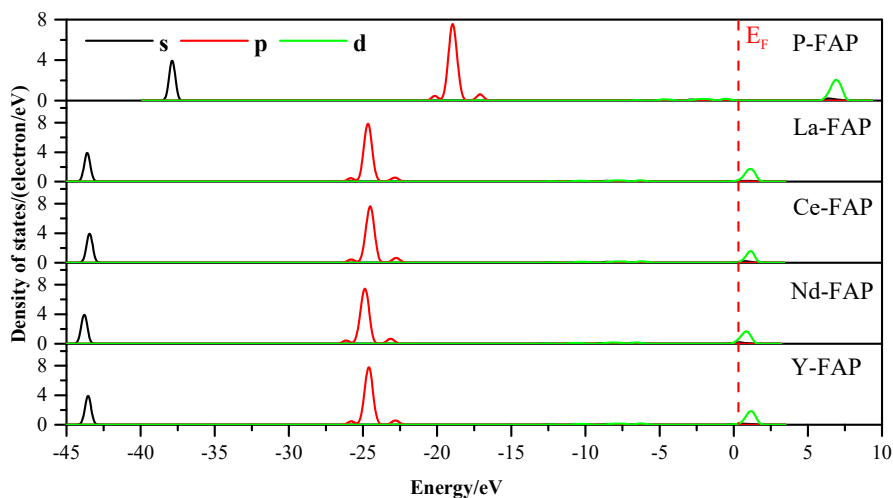


Figure 7. PDOS of a single Ca atom adjacent to the rare earth atom in REE-FAP crystals.

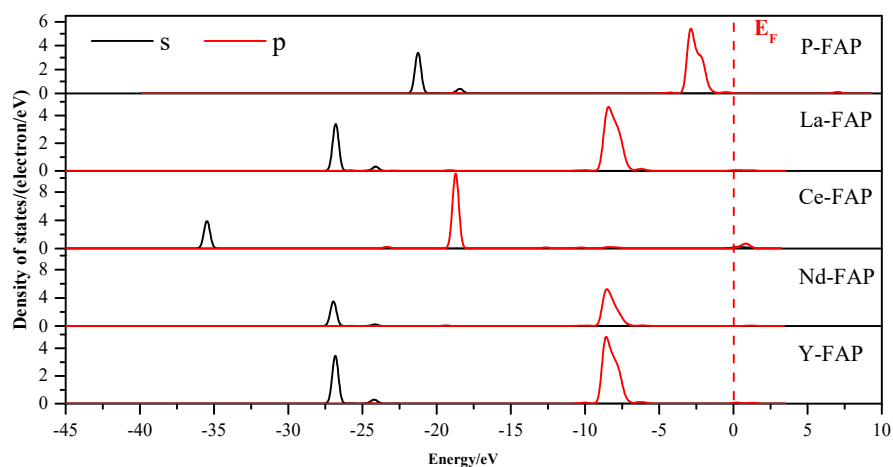


Figure 8. PDOS of a single F atom adjacent to the rare earth atom in REE-FAP crystals.

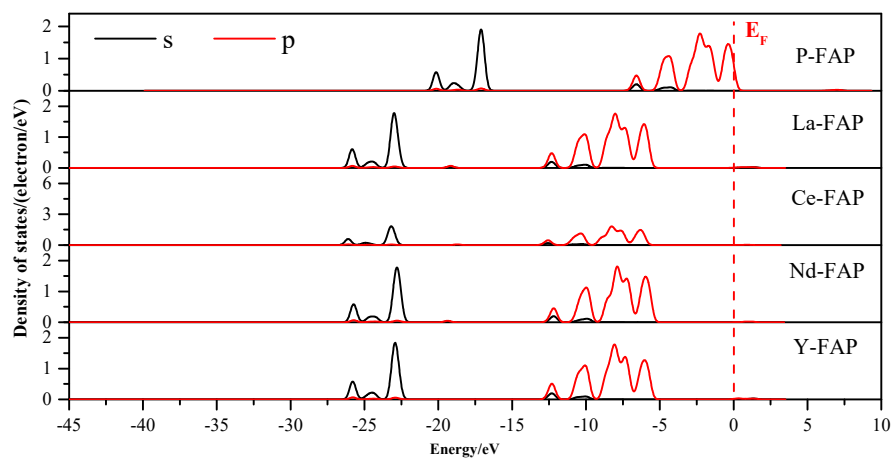


Figure 9. PDOS of a single O atom adjacent to the rare earth atom in REE-FAP crystals.

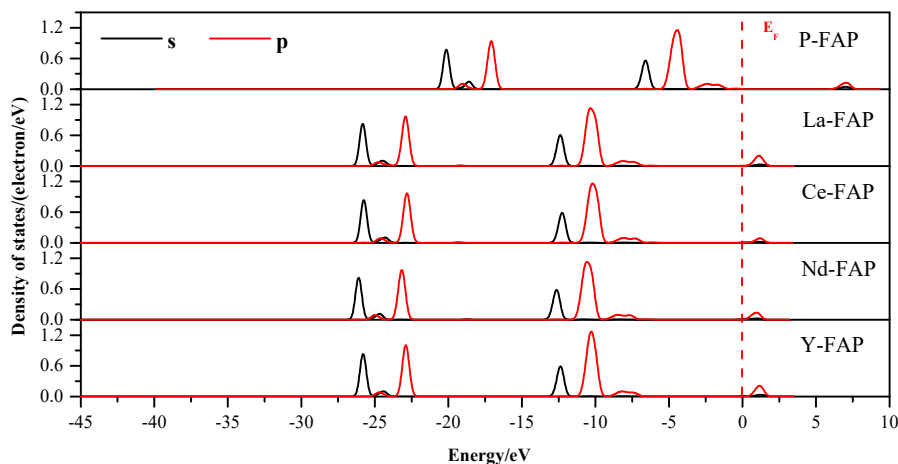


Figure 10. PDOS of a single P atom adjacent to the rare earth atom in REE-FAP crystals.

3.4. Analysis of the Mulliken Population

The Mulliken atomic charges population is an efficient method to describe the charge transfer, and the Mulliken bond population can also estimate the covalency and ionic strength of a chemical bond well [26]. A high value of the bond population indicates a covalent bond, while a low value indicates an ionic interaction. It has been reported that the atoms substituted in mineral crystals may affect the electronic properties of atoms closed to it [29,30,33]. So, the Mulliken populations of atoms and bonds adjacent to the REE atom in REE-FAP crystals were investigated comprehensively in Tables 2 and 3.

Table 2. Mulliken population of REE atom and the atoms adjacent to REE atom in REE-FAP crystals.

Defect Type	Species	Population				Total	Charge/e
		s	p	d	f		
P-FAP	Ca2	2.13 (−0.13)	6.00 (0)	0.51 (1.49)	0	8.64	1.36
	F	1.96 (0.04)	5.74 (−0.74)	0	0	7.70	−0.70
	O1	1.86 (0.14)	5.21 (−1.21)	0	0	7.07	−1.07
La-FAP	La	2.09 (−0.09)	6.10 (−0.10)	1.40 (0.60)	0	9.60	1.21
	F	1.96 (0.04)	5.72 (−0.72)	0	0	7.68	−0.68
	O1	1.86 (0.14)	5.16 (−1.16)	0	0	7.02	−1.02
Ce-FAP	Ce	2.15 (−0.15)	6.09 (−0.09)	0.79 (1.21)	1.65 (0.35)	10.67	1.32
	F	1.95 (0.05)	5.72 (−0.72)	0	0	7.67	−0.67
	O1	1.86 (0.14)	5.16 (−1.16)	0	0	7.02	−1.02
Nd-FAP	Nd	2.09 (−0.09)	6.06 (−0.06)	0.77 (1.23)	3.86 (0.14)	12.85	1.22
	F	1.95 (0.05)	5.71 (−0.71)	0	0	7.66	−0.66
	O1	1.86 (0.14)	5.16 (−1.16)	0	0	7.02	−1.02
Y-FAP	Y	0.16 (1.84)	0.09 (−0.09)	1.57 (−0.43)	0	1.82	1.32
	F	1.96 (0.04)	5.72 (−0.72)	0	0	7.68	−0.68
	O1	1.86 (0.14)	5.15 (−1.15)	0	0	7.01	−1.01

Note: The positive and negative numbers in parentheses represent the values of lost and derived electrons, respectively.

Results of Table 2 indicate that the p orbital of Ca2 atoms in the P-FAP crystal did not participate in the bonding, but the d orbital acted as the main electron donor, losing 1.49 e. The p orbital of F and O obtained electrons (−0.74 e and −1.21 e), and the s orbital lost electrons (0.04 e and 0.14 e), respectively, and both of F and O1 atoms were negatively charged because of obtaining electrons. By comparing REE-FAP with P-FAP, it can be seen that the substitution of REE led to the redistribution of atomic valence and charge in fluorapatite crystals. Consistent with the performance of Ca2 atoms, all REE atoms lost electrons in varying degrees, and were positively charged as a whole, and the charge was less than that of replaced Ca2 atoms. Among the four REEs, La, Ce and Nd mainly lost electrons in

the d orbital (0.60 e, 1.21 e and 1.23 e), while a small number of electrons were obtained in the s and p orbitals. The Y atom mainly lost electrons in the s orbital (1.84 e) while d orbital gained electrons (−0.43 e). The presence of REE increases the charge values of F and O1 atoms in both four REE-FAPs.

Table 3. Mulliken population of bonds formed between the REE atom and the atoms adjacent to the REE atoms in REE-FAP crystals.

Defect Type	Bond	Population	Bond Length/nm
P-FAP	Ca2–F	0.10	0.2327
	Ca2–O1	0.13	0.2363
	Ca2–O2	0.11	0.2385
	Ca2–O3	0.08	0.2478
La-FAP	La–F	0.11	0.2514
	La–O1	0.23	0.2447
	La–O2	0.19	0.2563
	La–O3	0.08	0.2590
Ce-FAP	Ce–F	0.13	0.2577
	Ce–O1	0.17	0.2461
	Ce–O2	0.14	0.2560
	Ce–O3	0.09	0.2709
Nd-FAP	Nd–F	0.15	0.2502
	Nd–O1	0.22	0.2474
	Nd–O2	0.16	0.2613
	Nd–O3	0.11	0.2703
Y-FAP	Y–F	0.17	0.2507
	Y–O1	0.30	0.2416
	Y–O2	0.23	0.2502
	Y–O3	0.15	0.2576

Table 3 shows the Mulliken population values of the bonds formed by the REE atoms and adjacent atoms in REE-FAP crystals. The occurrence of REE atoms increased both the population values and bond lengths of REE–F and REE–O bonds compared to Ca2–F and Ca2–O bonds in P-FAP crystal, indicating that the covalency of REE-bearing fluorapatite crystal was improved. This result was consistent with the literature research for structural analysis of calcium and lanthanum phosphosilicate apatites by Rietveld refinement [18], and similar with research for crystal chemistry of Th in fluorapatite [15]. Many studies have shown that the metal atom Ca has a certain number of unsaturated bonds and plays a key role on the common exposed surface of fluorophosphate ash [22,23]. Since REE–O was more covalent than Ca–O, the rare earth atom with unsaturated bond exposed on the surface of REE-FAP will interact with oleate much more intensely compared to the P-FAP. Therefore, the higher the covalent value, the stronger the adsorption capacity of oleic acid on the mineral surface will be [31]. From the above comprehensive analysis of the Mulliken population, the existence of REEs substitution may be in favor of the fluorapatite flotation.

3.5. Effect of Impurity on the Reactivity of Fluorapatite

The results of the above electronic structure showed that the REEs in the fluorapatite crystals change the crystal structure and electronic structure to varying degrees, such as unit cell parameters, Fermi level, density of states, Mulliken population and so on. Since the interaction of flotation reagents with minerals was affected by these factors, it may have an impact on the ability to obtain electrons of fluorapatite, and then affect its reactivity with oleic acid (OA).

The frontier orbital theory is a molecular orbital theory proposed by Fukui Kenichi in the 1950s [46], which can be used to describe the interaction between minerals and organic agents [31]. It is known that many properties of molecules are mainly caused by the frontier orbitals in the molecule, namely the

highest occupied molecular orbital (HOMO) and the lowest unoccupied molecular orbital (LUMO) decision. In the molecule, since HOMO has the highest electron energy and the least binding, it is the most active and most volatile, while LUMO has the lowest energy in all unoccupied orbits and tends to accept electrons. Therefore, these two orbitals determine the ability to gain and lose electrons in the molecule, and also determine important chemical properties such as the spatial orientation of the interaction of mineral with organics.

In the flotation, OA often acted by combining with calcium atoms on the surface of fluorapatite to form calcium oleate [34–37]. In this chemical interaction process, the HOMO of OA as an electron donor loses electrons, while the LUMO of fluorapatite as an electron acceptor gets electrons. According to frontier orbital theory, the absolute value of the difference between HOMO energy of one molecule and LUMO energy of another molecule can be used to characterize the interaction between them. Therefore, the interaction between fluorapatite and OA can be described by the following equation:

$$\Delta E = E_{\text{HOMO}}^{\text{OA}} - E_{\text{LUMO}}^{\text{FA}} \quad (2)$$

where the $E_{\text{HOMO}}^{\text{OA}}$ is the HOMO level of the OA, and $E_{\text{LUMO}}^{\text{FA}}$ is the LUMO level of fluorapatite.

According to the frontier orbital theory, the smaller the $|\Delta E|$ value, the stronger the interaction between the two [25]. Table 4 lists the HOMO and LUMO values of perfect fluorapatite, the REE-bearing fluorapatite, and $|\Delta E|$ values.

Table 4. Frontier orbital energies of the REE-FAP crystals and OA.

Defect Type	$E_{\text{HOMO}}/\text{eV}$	$E_{\text{LUMO}}/\text{eV}$	$ \Delta E /\text{eV}$
P-FAP	−7.059	−1.518	4.096
La-FAP	−7.233	−2.050	3.566
Ce-FAP	−1.987	−1.731	3.883
Nd-FAP	−2.898	−1.688	3.856
Y-FAP	−7.074	−1.639	3.975
OA	−5.614	−0.942	−

Table 4 shows that the REE atoms in the fluorapatite lattice changed the LUMO level of fluorapatite, that is to say, strengthened the ability of acquiring electrons when reacted with OA. Compared to P-FAP, the values of LUMO level of La-FAP, Ce-FAP, Nd-FAP and Y-FAP are reduced 0.532 eV, 0.213 eV, 0.170 eV, and 0.121 eV, respectively from −1.518 eV. The influence of REE substitution on the LUMO orbital of fluorapatite crystal was La > Ce > Nd > Y. The $|\Delta E|$ between perfect fluorapatite and OA was 4.096 eV. For the rare earth substituted fluorapatite system, the smaller the $|\Delta E|$ was, the more favorable the interaction between fluorapatite and OA was. Among the four REEs La, Ce, Nd and Y, the $|\Delta E|$ value of La-FAP was the smallest, which decreased from 4.096 eV of P-FAP to 3.566 eV, indicating that the interaction between La-FAP and OA will be the strongest.

4. Conclusions

The electronic structures of bulk fluorapatite bearing La, Ce, Nd and Y impurities were calculated using DFT, and their influence on the flotation behavior of fluorapatite were discussed using frontier molecular orbital theory. The results suggested that the REEs changed the structure and electronic properties of fluorapatite, including lattice parameters, Fermi Level, density of states and Mulliken population. The REEs impurities could change the energy value of the frontier orbital of fluorapatite. These impurities could also influence the reactivity of fluorapatite and consequently influence the interaction of fluorapatite with flotation collector, such as oleic acid. It is expected that the findings in these studies would help provide a new understanding of the influence of REEs on the electronic structures and floatability of fluorapatite, and also provide some theoretical basis for computation material for apatite doping REEs.

Author Contributions: X.W. and Q.Z. conceived and designed the calculation models; Q.Z. contributed the computation resources; X.W. performed all the calculations and wrote the original manuscript; S.M. and W.C. participated in the data analysis and manuscript modification.

Funding: This work was financially supported by the National Natural Science Foundation of China (U1812402 and 51474078) and Guizhou Provincial Science and Technology Foundation (Qian Ke He J-(2015)-2048).

Conflicts of Interest: The authors declare no conflict of interest.

References

1. Connelly, N.G.; Damhus, T.; Hartshorn, R.M.; Hutton, A.T. *Nomenclature of Inorganic Chemistry: IUPAC Recommendations 2005*; RSC Publishing: Cambridge, UK, 2005.
2. Chen, Z.H. Global rare earth resources and scenarios of future rare earth industry. *J. Rare Earths* **2011**, *29*, 1–6. [[CrossRef](#)]
3. Zhou, B.L.; Li, Z.X.; Chen, C.C. Global potential of rare earth resources and rare earth demand from clean technologies. *Minerals* **2017**, *7*, 203. [[CrossRef](#)]
4. Massari, S.; Ruberti, M. Rare earth elements as critical raw materials: Focus on international markets and future strategies. *Resour. Policy* **2013**, *38*, 36–43. [[CrossRef](#)]
5. Jordens, A.; Cheng, Y.P.; Waters, K.E. A review of the beneficiation of rare earth element bearing minerals. *Miner. Eng.* **2013**, *41*, 97–114. [[CrossRef](#)]
6. Edahbi, M.; Plante, B.; Benzaazoua, M.; Kormos, L.; Pelletier, M. Rare earth elements (La, Ce, Pr, Nd, and Sm) from a carbonatite deposit: Mineralogical characterization and geochemical behavior. *Minerals* **2018**, *8*, 55. [[CrossRef](#)]
7. Wu, S.X.; Wang, L.S.; Zhao, L.S.; Zhang, P.; El-Shall, H.; Moudgil, B.; Huang, X.W.; Zhang, L.F. Recovery of rare earth elements from phosphate rock by hydrometallurgical processes—A critical review. *Chem. Eng. J.* **2018**, *335*, 774–800. [[CrossRef](#)]
8. Jin, H.X.; Wu, F.Z.; Mao, X.H.; Wang, M.L.; Xie, H.Y. Leaching isomorphism rare earths from phosphorite ore by sulfuric acid and phosphoric acid. *Rare Met.* **2017**, *36*, 840–850. [[CrossRef](#)]
9. Wang, J.R.; Zhang, J. Study on the selective leaching of Low-Grade phosphate ore for beneficiation of phosphorus and rare earths using citric acid as leaching agent. *Russ. J. Appl. Chem.* **2016**, *89*, 1196–1205.
10. Chen, J.Y.; Yang, R.D.; Wei, H.R.; Gao, J.B. Rare earth element geochemistry of Cambrian phosphorites from the Yangtze Region. *J. Rare Earths* **2013**, *31*, 101–112. [[CrossRef](#)]
11. Li, S.; Zhang, J.; Wang, H.F.; Wang, C.L. Geochemical characteristics of dolomitic phosphorite containing rare earth elements and its weathered ore. *Minerals* **2019**, *9*, 416. [[CrossRef](#)]
12. Roelandts, I. Determination of light rare earth elements in apatite by x-ray fluorescence spectrometry after anion exchange extraction. *Anal. Chem.* **1981**, *53*, 676–680. [[CrossRef](#)]
13. Ardanova, L.I.; Get'Man, E.I.; Loboda, S.N.; Prisedsky, V.V.; Tkachenko, T.V.; Marchenko, V.I.; Antonovich, V.P.; Chivireva, N.A.; Chebishev, K.A.; Lyashenko, A.S. Isomorphous substitutions of rare earth elements for calcium in synthetic hydroxyapatites. *Inorg. Chem.* **2010**, *49*, 10687–10693. [[CrossRef](#)] [[PubMed](#)]
14. Liu, Y.; Peng, M.S. Advances in the researches on structural substitution of apatite. *Acta Petrol. Mineral. (Chin.)* **2003**, *22*, 413–415.
15. Luo, Y.; Rakovan, J.; Tang, Y.; Lupulescu, M.; Hughes, J.M. Crystal chemistry of Th in fluorapatite. *Am. Mineral.* **2011**, *96*, 23–33. [[CrossRef](#)]
16. Fleet, E.M.; Pan, Y.M. Site preference of rare earth elements in fluorapatite. *Am. Mineral.* **1995**, *80*, 329–335. [[CrossRef](#)]
17. Fleet, E.M.; Pan, Y.M. Site preference of rare earth elements in fluorapatite: Binary (LREE + HREE)-substituted crystals. *Am. Mineral.* **1997**, *82*, 870–877. [[CrossRef](#)]
18. Njema, H.; Boughzala, K.; Boughzala, H.; Bouzouita, K. Structural analysis by Rietveld refinement of calcium and lanthanum phosphosilicate apatites. *J. Rare Earths* **2013**, *31*, 897–904. [[CrossRef](#)]
19. Hughes, M.J.; Cameron, M. Rare-earth-element ordering and structural variations in natural rare-earth bearing apatites. *Am. Mineral.* **1991**, *76*, 1165–1173.
20. Fleet, E.M.; Pan, Y. Crystal chemistry of rare earth elements in fluorapatite and some calc-silicates. *Eur. J. Miner.* **1995**, *7*, 591–605. [[CrossRef](#)]

21. De Leeuw, N.H. Density functional theory calculations of solid solutions of fluor- and chlorapatites. *Chem. Mater.* **2002**, *14*, 435–441. [[CrossRef](#)]
22. Qiu, Y.Q.; Cui, W.Y.; Li, L.J.; Ye, J.J.; Wang, J.; Zhang, Q. Structural, electronic properties with different terminations for fluorapatite (0 0 1) surface: A first-principles investigation. *Comp. Mater. Sci.* **2017**, *126*, 132–138. [[CrossRef](#)]
23. Rulis, P.; Yao, H.Z.; Ouyang, L.Z.; Ching, W.Y. Electronic structure, bonding, charge distribution, and x-ray absorption spectra of the (0 0 1) surfaces of fluorapatite and hydroxyapatite from first principles. *Phys. Rev. B* **2007**, *76*, 245410. [[CrossRef](#)]
24. Wang, X.C.; Zhang, Q.; Li, X.B.; Ye, J.J.; Li, L.J. Structural and electronic properties of different terminations for quartz (001) surfaces as well as water molecule adsorption on it: A First-Principles study. *Minerals* **2018**, *8*, 58. [[CrossRef](#)]
25. Xie, J.; Li, X.H.; Mao, S.; Li, L.J.; Ke, B.L.; Zhang, Q. Effects of structure of fatty acid collectors on the adsorption of fluorapatite (0 0 1) surface: A first-principles calculations. *Appl. Surf. Sci.* **2018**, *444*, 699–709. [[CrossRef](#)]
26. Chen, J.H. *The Solid Physics of Sulphide Minerals Flotation*; Central South University Press: Changsha, China, 2015.
27. Chen, J.H.; Ke, B.L.; Lan, L.H.; Li, Y.Q. DFT and experimental studies of oxygen adsorption on galena surface bearing Ag, Mn, Bi and Cu impurities. *Miner. Eng.* **2015**, *71*, 170–179.
28. Chen, J.H.; Ke, B.L.; Lan, L.H.; Li, Y.Q. Influence of Ag, Sb, Bi and Zn impurities on electrochemical and flotation behaviour of galena. *Miner. Eng.* **2015**, *72*, 10–16. [[CrossRef](#)]
29. Chen, Y.; Chen, J.H.; Guo, J. A DFT study on the effect of lattice impurities on the electronic structures and floatability of sphalerite. *Miner. Eng.* **2010**, *23*, 1120–1130. [[CrossRef](#)]
30. Chen, Y.; Chen, J.H.; Lan, L.H.; Yang, M.J. The influence of the impurities on the flotation behaviors of synthetic ZnS. *Miner. Eng.* **2012**, *27*, 65–71. [[CrossRef](#)]
31. Li, Y.Q.; Chen, J.H.; Chen, Y. Electronic structures and flotation behavior of pyrite containing vacancy defects. *Acta Phys. Chim. Sin.* **2010**, *26*, 1435–1441.
32. Chen, J.H.; Wang, L.; Chen, Y.; Guo, Y. Density functional theory of effects of vacancy defects on electronic structure and flotation of galena. *Chin. J. Nonferr. Met.* **2010**, *20*, 1815–1821.
33. Gao, Z.; Sun, W.; Gao, J.; Hu, Y. A Density Functional Theory Study on the Effect of Lattice Impurities on the Electronic Structures and Reactivity of Fluorite. *Minerals* **2017**, *7*, 160.
34. Filippova, I.V.; Filippov, L.O.; Lafhaj, Z.; Barres, O.; Fornasiero, D. Effect of calcium minerals reactivity on fatty acids adsorption and flotation. *Colloids Surf. A Phys. Eng. Asp.* **2018**, *545*, 157–166. [[CrossRef](#)]
35. Owens, C.L.; Nash, G.R.; Hadler, K.; Fitzpatrick, R.S.; Anderson, C.G.; Wall, F. Apatite enrichment by rare earth elements: A review of the effects of surface properties. *Adv. Colloid Interface Sci.* **2019**, *265*, 14–28. [[CrossRef](#)] [[PubMed](#)]
36. Kou, J.; Tao, D.; Xu, G. Fatty acid collectors for phosphate flotation and their adsorption behavior using QCM-D. *Int. J. Miner. Process.* **2010**, *95*, 1–9. [[CrossRef](#)]
37. Paiva, P.R.P.; Monte, M.B.M.; Sim, O.R.A.; Gaspar, J.C. In Situ AFM study of potassium oleate adsorption and calcium precipitate formation on an apatite surface. *Miner. Eng.* **2011**, *24*, 387–395. [[CrossRef](#)]
38. Santos, E.P.; Dutra, A.; Oliveira, J.F. The effect of jojoba oil on the surface properties of calcite and apatite aiming at their selective flotation. *Int. J. Miner. Process.* **2015**, *143*, 34–38. [[CrossRef](#)]
39. Ye, J.J.; Zhang, Q.; Li, X.B.; Wang, X.C.; Ke, B.L.; Li, X.H.; Shen, Z.H. Effect of the morphology of adsorbed oleate on the wettability of a colophane surface. *Appl. Surf. Sci.* **2018**, *444*, 87–96. [[CrossRef](#)]
40. Hughes, M.J.; Cameron, M.; Crowley, K.D. Structural variations in natural F, OH, and Cl apatites. *Am. Mineral.* **1989**, *74*, 870–876.
41. Segall, M.D.; Lindan, P.J.D.; Probert, M.J.; Pickard, C.J.; Hasnip, P.J.; Clark, S.J.; Payne, M.C. First-principles simulation: Ideas, illustrations and the CASTEP code. *J. Phys. Condens. Matter* **2002**, *14*, 2717–2744. [[CrossRef](#)]
42. Vanderbilt, D. Soft self-consistent pseudopotentials in a generalized eigenvalue formalism. *Phys. Rev. B* **1990**, *41*, 7892–7895. [[CrossRef](#)]
43. Perdew, J.P.; Chevary, J.A.; Vosko, S.H.; Jackson, K.A.; Pederson, M.R.; Singh, D.J.; Fiolhais, C. Atoms, molecules, solids, and surfaces: Applications of the generalized gradient approximation for exchange and correlation. *Phys. Rev. B* **1992**, *46*, 6671–6687. [[CrossRef](#)] [[PubMed](#)]

44. Ferrer, I.J.; De La Heras, C.; Sanchez, C. The effect of Ni impurities on some structural properties of pyrite thin films. *J. Phys. Condens. Matter* **1995**, *7*, 2115–2121. [[CrossRef](#)]
45. Imai, Y.; Mukaida, M.; Tsunoda, T. Calculation of electronic energy and density of state of iron-disilicides using a total-energy pseudopotential method, CASTEP. *Thin Solid Films* **2001**, *381*, 176–182. [[CrossRef](#)]
46. Yamabe, S.; Minato, T. Frontier orbital theory. *J. Chem. Educ.* **1992**, *40*, 450–454.



© 2019 by the authors. Licensee MDPI, Basel, Switzerland. This article is an open access article distributed under the terms and conditions of the Creative Commons Attribution (CC BY) license (<http://creativecommons.org/licenses/by/4.0/>).